



# 1 Winter hydrometeorological extreme events modulated by 2 large scale atmospheric circulation in southern Ontario

3 Olivier Champagne<sup>1\*</sup>, Martin Leduc<sup>2</sup>, Paulin Coulibaly<sup>1,3</sup>, M. Altaf Arain<sup>1</sup>

4 1 School of Geography and Earth Sciences, McMaster University, Hamilton, Ontario, Canada

5 2 Ouranos and Centre ESCER, Université du Québec à Montréal, Montréal, Québec, Canada

6 3 Department of Civil Engineering, McMaster University, Hamilton, Ontario, Canada

7 Correspondence to: Olivier Champagne (champago@mcmaster.ca)

8 **Abstract.** Extreme events are widely studied across the world because of their major implications for many  
9 aspects of society and especially floods. These events are generally studied in term of precipitation or temperature  
10 extreme indices that are often not adapted for regions affected by floods caused by snowmelt. Rain on Snow index  
11 has been widely used but it neglects rain only events which are expected to be more frequent in the future. In this  
12 study we identified a new winter compound index and assessed how large-scale atmospheric circulation controls  
13 the past and future evolution of these events in the Great Lakes region. The future evolution of this index was  
14 projected using temperature and precipitation from the Canadian Regional Climate Model Large Ensemble  
15 (CRCM5-LE). These climate data were used as input in PRMS hydrological model to simulate the future evolution  
16 of high flows in three watersheds in Southern Ontario. We also used five recurrent large-scale atmospheric  
17 circulation patterns in northeastern North America and identified how they control the past and future variability  
18 of the newly created index and high flows. The results show that daily precipitation higher than 10mm and  
19 temperature higher than 5°C were a necessary historical condition to produce high flows in these three watersheds.  
20 In the historical period, the occurrences of these heavy rain and warm events as well as high flows were associated  
21 to two main patterns characterized by high Z500 anomalies centred on eastern Great Lakes (HP) and the Atlantic  
22 Ocean (South). These hydrometeorological extreme events will be more frequent in the near future and will still  
23 be associated to the same atmospheric patterns. The future evolution of the index will be modulated by the internal  
24 variability of the climate system as higher Z500 in the east coast will amplify the increase in the number of events,  
25 especially the warm events. The relationship between the extreme weather index and high flows will be modified  
26 in the future as the snowpack reduces and rain becomes the main component of high flows generation. This study  
27 shows the values of CRCM5-LE dataset to simulate hydrometeorological extreme events in Eastern Canada and  
28 to better understand the uncertainties associated to internal variability of climate.



## 29 **1 Introduction**

30 According to the actual pathway of greenhouse gases emissions, temperature will continue to rise in the future  
31 with serious implications for society (Hoegh-Guldberg et al., 2018). The amount of precipitation, especially for  
32 extreme events, is also projected to increase globally (Kharin et al., 2013), due to the acceleration of the  
33 hydrological cycle (Trenberth, 1999). Because extreme precipitation has a great societal impact across the world,  
34 internationally coordinated climate indices, built from precipitation and temperature data, are widely used to  
35 assess the evolution of different weather extremes (Zhang et al., 2011). Some of these indices such as monthly or  
36 annual maximum of precipitation can be used to improve flood management. However, in catchments that receive  
37 snowfall, a large number of floods may occur due to a combination of temperature and precipitation extreme  
38 events such as Rain on Snow (ROS) (Merz and Blöschl, 2003). The impact of ROS on floods generation have  
39 been widely studied in different regions of the world, including Central Europe (Freudiger et al., 2014), the Alps  
40 (Würzer et al., 2016), the Rocky mountains (Musselman et al., 2018) or the New York State (Pradhanang et al.,  
41 2013). The projections of these events can be a challenge because they depend on the ability of the climate model  
42 to project the precipitation extremes and the aerial extent of snowmelt (McCabe et al., 2007). The climate models  
43 improvements allowed recent studies to project the future evolution of ROS (Il Jeong and Sushama, 2018;  
44 Musselman et al., 2018; Surfleet and Tullos, 2013). However strong uncertainties in the projections of such events  
45 remains, especially due to the internal variability of climate (Lafaysse et al., 2014). These uncertainties, even with  
46 the perfect climate model, will never be eradicated due to the inherently chaotic characteristic of the atmosphere  
47 (Lorenz, 1963, Deser, 2014). ROS are clearly controlled by large scale atmospheric circulation (Cohen et al.,  
48 2015) emphasizing the need to include internal climate variability uncertainties in the future evolution of ROS  
49 studies. The Great Lakes region is one of the area of the world highly impacted by ROS events in winter (Buttle  
50 et al., 2016; Cohen et al., 2015). In this region, previous studies found correlations between precipitation and  
51 temperature extremes and large-scale circulation indices: The negative phase of the pacific North America  
52 oscillation (PNA) brings more heavy precipitation events in the region south of Great Lakes region (Mallakpour  
53 and Villarini, 2016; Thiombiano et al., 2017) and more snowfall in the region North of Great Lakes (Zhao et al.,  
54 2013), due to high moisture transport over the region (Mallakpour and Villarini, 2016). Another study showed a  
55 negative phase of PNA and positive phase of North Atlantic Oscillation (NAO) associated with warm days (Ning  
56 and Bradley, 2015). Temperature and precipitation uncertainties associated to climate internal variability have  
57 also been assessed in North America using a global climate model large ensemble (GCM-LE) (Deser et al., 2014).  
58 These studies generally separate precipitation and temperature while studying compound events, such as ROS,  
59 has been preconized recently to improve our understanding of extreme impacts (Leonard et al., 2014). The



60 definition of ROS index is also subjected to high uncertainties (Kudo et al., 2017) and this index may not be  
61 relevant in regions affected by decrease of snowpack (Il Jeong and Sushama, 2018). These results emphasize the  
62 need of new compound climate indices to understand the impact of atmospheric circulation on  
63 hydrometeorological extreme events in the Great lake region. In this study, CRCM5-LE, a 50-member regional  
64 model ensemble at a 12km resolution produced over northeastern North America, will be used with the following  
65 objectives:

66

67 (1) Define a regional precipitation and temperature compound index that contributes to winter high flows in  
68 Southern Ontario, which is the most populated area in the Great Lakes region.

69 (2) Assess the relationship between the occurrence of this index and the past large-scale atmospheric circulation.

70 (3) Investigate the pertinence of the index to explain the future evolution of projected high flows and

71 (4) Demonstrate how internal variability of climate will modulate the future evolution of atmospheric circulation  
72 and number of hydrometeorological extreme events in the region.

## 73 **2 Data and methods**

### 74 **2.1 Climate data**

75 Observations of precipitation, minimum temperature and maximum temperature for the winter months (DJF) in  
76 the 1957-2012 period were taken from the gridded historical weather station data (CanGRD) produced by  
77 McKenney *et al.*, (2011). These data were generated from an interpolation of Natural Resources Canada and  
78 Environment and Climate Change Canada (ECCC) data archives at 10 km spatial resolution. The simulated  
79 evolution of precipitation and temperature are from the Canadian Regional Climate Model Large Ensemble  
80 (CRCM5-LE). CRCM5-LE is a 50-member regional model ensemble at 12km resolution produced over  
81 northeastern North America in the scope of the Québec-Bavaria international collaboration on climate change  
82 (ClimEx project; Leduc et al., 2019). CRCM5-LE is the downscaled version of the global Canadian model large  
83 ensemble (CanESM2-LE) at 310km resolution and offers the possibility to relate each member of CRCM5-LE to  
84 its corresponding member in CanESM2-LE. The future climate data have been bias corrected following the  
85 method of Ines and Hansen (2006) and using the observations and CRCM5-LE historical data in the 1957-2012  
86 period. For each month of the year, the intensity distribution of temperature was corrected using a normal  
87 distribution while the precipitation frequency and intensity distribution were corrected with a gamma distribution.  
88 Each CRCM5-LE grid point has been bias corrected using the closest CanGRD point. Using a unique CanGRD



89 point for each CRCM5-LE point is permitted in our study because of low elevation gradients between points, the  
90 spatial variability of temperature and precipitation being more dependent on the proximity of the Lakes than the  
91 elevation (Scott and Huff, 1996).

## 92 **2.2 Heavy rain and warm index**

93 Streamflow observations from three watersheds in southern Ontario (Figure 1) were used to define the daily  
94 temperature and precipitation threshold needed to generate high flows in winter. A high flow event was defined  
95 for each watershed as streamflow higher than a threshold equal to the mean streamflow plus three times the  
96 standard deviation. When more than two days in a row were higher than the high flow threshold, the event was  
97 considered as a single event and only the day with the highest high flow was considered. Figure 2 shows for each  
98 high flow event the distribution of daily temperature and precipitation amounts from all grids of the watersheds.  
99 The precipitation and temperature data are from the day situated two days before the high flow event for Big  
100 Creek watershed and three days before the high flow event for Thames and Grand rivers. This lag corresponds to  
101 the delay between a rainfall and/or warm event and the peak flow at the outlet. Figure 2 shows a maximum  
102 temperature higher than 5°C and precipitation higher than 10mm for most grid points during the high flow events.  
103 These temperature and precipitation thresholds are used to create the new index and define days with a significant  
104 rain and warm event that has the potential to generate a high flow event. The 5°C threshold gives a strong  
105 indication that precipitation is in a form of rain, and that the snow in the ground is melting. This index is similar  
106 to the Rain on Snow index (ROS) defined by previous studies. The threshold of 10 mm was previously used to  
107 define ROS events with floods potential (Cohen et al., 2015; Musselman et al., 2018). Our newly created index  
108 can be defined rather as a heavy rain and warm index because snowpack is not integrated in the calculation.

## 109 **2.3 Hydrological modelling**

110 The future evolution of high flows in the three watersheds have been simulated using the Precipitation Runoff  
111 Modeling System (PRMS). PRMS is a semi distributed conceptual hydrological model widely used in snow  
112 dominated regions (Dressler et al., 2006; Liao and Zhuang, 2017; Mastin et al., 2011; Surfleet et al., 2012; Teng  
113 et al., 2017, 2018). PRMS computes the water flowing between hydrological reservoirs (plan canopy interception,  
114 snowpack, soil zone, subsurface) for each hydrological response unit (HRU). For a general description of PRMS  
115 the reader is referred to Markstrom *et al.*, (2015). Champagne *et al.*, (2019) previously applied PRMS to these  
116 three watersheds and extensively described the parametrization process. PRMS has been calibrated in the 1989-  
117 2009 period using Precipitation, minimum temperature and maximum temperature from CanGRD. The three step



118 trial-and-error calibration approach applied to each watershed showed satisfactory results (Champagne *et al.*,  
119 2019). The streamflow was simulated for each member of the ensemble in the 1957-2055 period using CMIP5-  
120 LE bias corrected data described in the section 2.1.

## 121 **2.4 Atmospheric circulation patterns**

122 The recurrent atmospheric patterns in northeastern North-America were identified by a weather regimes technique  
123 computed by a k-means algorithm (Michelangeli *et al.*, 1995). The algorithm used daily geopotential height  
124 anomalies at 500hPa level (Z500) from the 20<sup>th</sup> century reanalyses (20thCR, Compo *et al.*, 2011) and was applied  
125 in the 1957-2012 period to the northeastern part of North America (30 N-60 N/110 W-50 W). Prior to the k-means  
126 calculations we identified the principal components of the Z500 maps that explain 80% of the spatial variance.  
127 These principal components have been decomposed in weather regimes thanks to the k-means algorithm. k-means  
128 creates the classes by an iteration method that minimizes intra-regime Euclidean distance and maximize inter-  
129 regime Euclidean distance between the principal components of each day. The algorithm is repeated 100 times  
130 for each number of class between 2 and 10. The choice of the final class number is decided by a red noise test.  
131 This test consists in assessing the significance of the decomposition against weather regimes calculated from 100  
132 randomly generated theoretical datasets that have the same statistical properties than the original dataset. The  
133 weather regimes have been previously calculated for the same domain and the red noise test shows five classes as  
134 the most robust choice (Champagne *et al.*, 2019).

135

136 The principal components corresponding to these five classes calculated with 20thCR have been used by the k-  
137 means algorithm to create similarly five weather regimes for each member of CanESM2-LE. The weather regimes  
138 calculated with CanESM2-LE have been calculated in two periods of similar length 1957-2012 and 2013-2068.  
139 Z500 anomalies from CanESM2-LE have been calculated separately for these two periods to avoid a large climate  
140 change signal in the evolution of regime occurrences. The variability of regime occurrences due to internal  
141 variability of climate is therefore fully preserved.

## 142 **3 Results**

### 143 **3.1 Weather regimes in northeastern North America**

144 Five weather regimes have been identified in northeastern North America according to the red noise test and show  
145 distinct weather patterns (Figure 3). The weather regimes computed with 20thCR data show two clear opposite



146 patterns characterized by positive (HP) and negative (LP) geopotential height anomalies on the Great Lakes. The  
147 regime South was characterized by positive Z500 anomalies in the Atlantic Ocean and negative anomalies in the  
148 north-west part of the domain and was associated with southerly winds. The regime North-West had low  
149 geopotential height on the Gulf of Saint-Lawrence together with winds from the northwest over the Great Lakes  
150 region. Finally, the regime North-East was associated with low geopotential height in the Atlantic Ocean but high  
151 geopotential height close to the Arctic that drove northeastern winds over the Great Lakes. The weather regimes  
152 calculated with CanESM2-LE data in the historical period have very similar patterns (Figure 3). CanESM2 50  
153 members average Z500 anomalies were generally less strong than the 20thCR weather regimes and the anomalies  
154 were slightly shifted to the South. The Z500 anomalies over the Great Lakes were similar for most of the regime  
155 except for regime South showing higher Z500 anomalies.

### 156 **3.2 Validation of heavy rain and warm index and high flows simulated by CRCM5-LE**

157 The ability of CRCM5-LE to simulate the occurrence of heavy rain and warm events is assessed in this section.  
158 The number of heavy precipitation events per winter was generally well recreated by the regional ensemble in the  
159 historical period (Figure 4). These events were generally overestimated in the north and western parts of the region  
160 especially in areas close to Lake Huron. In this region, few grid points show all 50 members of the ensemble  
161 overestimating the number of events compared to the observations. The number of warm events followed a similar  
162 spatial variability with more frequent events in the southern parts, particularly in the Niagara peninsula between  
163 Lake Erie and Lake Ontario. The number of warm events was overestimated by all members in the entire area  
164 except for the Lake Simcoe Area (Figure 4 Centre-right plot in blue). The number of compound events, heavy  
165 rain and warm temperature was more frequent in the area close to Lake Erie in both observations and simulations.  
166 The number of events was overestimated by the ensemble mean in the northern parts of the region. In this region,  
167 many grid points show all members of the ensemble overestimating the number of events. Close to Lake Erie the  
168 overestimation was lower and even non-existent in the Niagara peninsula.

169

170 The ability of the ensemble to recreate the number of heavy rain and warm events relative to the number of  
171 occurrences of each weather regime has been assessed for the heavy precipitation events, the warm events and the  
172 compound events. For the heavy precipitation events the observations show high number of events during the  
173 occurrence of regimes HP in the southern parts of the region and especially in inland areas (Figure 5). The regime  
174 South show the second largest number of heavy precipitation events while the regime North-West was associated  
175 with the least number of heavy precipitation events. The number of precipitation events associated to a regime LP



176 is spatially variable with a large number of events limited to the Lake Huron shoreline. The ensemble appeared to  
177 recreate with accuracy these number of events per weather regimes. The regime South is the exception with almost  
178 twice more events per occurrence of regime with the 50 members average compared to OBS. In southern areas  
179 the simulations were also slightly overestimating the number of heavy precipitation events during regime North-  
180 West while underestimating during regime HP (Figure 5).

181

182 Concerning the observed warm events, they also occurred mostly during regime HP while they were non-existent  
183 during regime LP (Figure 6). The number of warm events was similar between regimes North-West, North-East  
184 and South in a large part of the area. In the Niagara peninsula more events were occurring during a regime South.  
185 The simulations recreated well the number of warm events for the regimes HP, LP and North-East while it  
186 overestimated the number of events for the two other regimes and especially the regime South (Figure 6). The  
187 number of events per occurrence of regime South for the 50 members average was twice the number of events  
188 calculated with the observations.

189

190 The compound index heavy rain and warm events was also more frequent during a regime HP in both observations  
191 and simulations while the occurrences of events were very low for LP and North-West (Figure 7). The simulations  
192 overestimated these events by 3 to 4 times for the regime South while it was well recreated for the other regimes  
193 (Figure 7).

194

195 The historical distribution of streamflow associated to heavy rain and warm events for the observed streamflow  
196 (OBS), streamflow simulated with CanGRD (CTL) and streamflow simulated with each CRCM5-LE member  
197 (ENS) is shown in Figure 8. The results show an observed streamflow frequently higher than the high flows  
198 threshold when the heavy rain and warm events occurred during a regime HP. Few days also show high flows  
199 during a regime South especially in Thames River and Big Creek watersheds. The streamflow simulated with  
200 CanGRD weather data (CTL) is underestimated but show a similar inter-regime variability with higher streamflow  
201 during HP heavy rain and warm events compared to events associated with other weather regimes. The 50  
202 simulations from CRCM5-LE show also higher streamflow when heavy rain and warm events correspond to  
203 regimes HP or South (Figure 8).





### 204 **3.3 Future evolution in the number of hydrometeorological extreme events**

205 The total number of heavy precipitation events simulated by CRCM5-LE is expected to increase between 1961-  
206 1990 and 2026-2055, with a maximum increase between 1 and 2 events per winter expected close to the Georgian  
207 Bay (Figure 9). The increase in the number of events is mainly expected during the regime South but also for the  
208 regime LP near Lake Huron and HP between the Georgian Bay and Lake Ontario. The increased frequency of  
209 warm events is expected to be even higher reaching a total increase of about 10 events close to Lake Erie. The  
210 highest increase is expected for HP regime and at a lower rate for regimes South and North-West. The number of  
211 compound events is expected to increase by 1 or 2 events per winter with a maximal increase between Lake Erie  
212 and Huron. The increase in the number of heavy rain and warm events is expected to concern mainly the regime  
213 South and HP (Figure 9).

214

215 The contribution of the trend in heavy rain and warm events to the trend in number of high flows has been  
216 investigated (Figure 10). For each member of the ensemble, the historical number of high flows events associated  
217 to each weather regime has been multiplied by the change factor between number of Rain and warm events in the  
218 historical period and in the future period. The difference between this calculated number of high flows and the  
219 historical number of high flows corresponds to the theoretical high flows frequency change due to the occurrence  
220 change in number of heavy rain and warm events (OCC). The total change in number of high flows (TOT)  
221 corresponding to each weather regimes is subtracted by OCC for each ensemble member to account for a change  
222 in number of high flows not due to a change in number of heavy rain and warm events (DIF). Taking all weather  
223 regimes events together, TOT is expected to increase in the future. The increase in OCC is similar to the increase  
224 in TOT even though OCC is slightly higher than TOT in the Big Creek watershed. Considering HP's events only,  
225 the increase of OCC is higher than TOT while for events associated with regime South TOT is higher than OCC.

### 226 **3.4 Relationship between change in occurrence of weather regimes and extreme events**

227 Correlations between change of occurrence of weather regimes and change in number of Rain and Warm events  
228 between 1961-1990 and 2026-2055 for the 50 members have been calculated for each grid point (Figure 11). The  
229 correlations between occurrence of weather regimes and warm events is higher compared to correlations with  
230 heavy precipitation events. The results show positive correlations between warm events and regime HP and  
231 negative correlations between warm events and regime LP/North-east in the entire area. The change in number of  
232 warm events is also positively correlated to the change in occurrence of regime South but the results are not  
233 significance (95% confidence). The correlations with the compound index are less spatially spread with positive





234 correlations between the index and the regime HP close to Lake Erie and negative correlations with regime LP  
235 near Lake Huron.

236

237 Correlations between combination of weather regimes change and Rain and warm index change averaged over  
238 the entire region have also been investigated (Table 1). The combinations of weather regimes have been done by  
239 summing the change of occurrence from the two regimes of each combination. The correlations between change  
240 of any weather regimes combinations and change in number of heavy precipitation events are not significant. The  
241 correlations between change of number of warm events and change in occurrence of weather regimes is improved  
242 when regime South is associated to regime HP and when regime LP is associated to regime NE compared to  
243 correlations with regimes HP or LP only (Table 1). Concerning the heavy rain and warm index the correlations  
244 are not significant if the regimes HP and South are correlated separately to the number of events but are positive  
245 and significant (95% confidence interval) if the correlation is applied to a combination of regime South-HP and  
246 negative and significant (90% confidence interval) with a combination of North-west-LP. The correlation with  
247 the high flows in each of the three watersheds have also been investigated (Table 2) and shows significance only  
248 in the Big Creek watershed. A combination of HP-LP is negatively correlated to high flows while North-west and  
249 a combination North-west-South are positively correlated to high flows.

250

251 The change of heavy precipitation, warm and compound events frequency in respect to change of occurrence of  
252 regimes South, HP, LP and North-west for each member of the ensemble is shown in Figure 12. The  
253 correspondence between change in number of heavy precipitations events and change in number of occurrences  
254 of weather regimes is not clear, confirming the low correlations in Figure 11 and Table 1. Regarding the warm  
255 events, the large increase in occurrence of regime HP-South or large decrease in regimes LP-North-West are  
256 generally associated to a large increase in number of warm events confirming the results from Figure 11 and Table  
257 1. Concerning the compound index, despite the correlations shown in Figure 11 and Table 1, a high increase of  
258 HP and South occurrences does not systematically lead to a large increase in number of events (Figure 12).

## 259 **4 Discussion**

### 260 **4.1 Atmospheric circulation and extreme weather events**

261 The results show that the occurrence of heavy rain and warm events are modulated by specific atmospheric  
262 patterns in winter which corroborates previous studies in the Great Lakes region. These studies found that heavy



263 precipitation and flooding events are associated to high geopotential height anomalies in the east coast of North  
264 America similarly to regimes HP or South (Mallakpour and Villarini, 2016; Zhang and Villarini, 2019; Farnham  
265 *et al.*, 2018)). Our results found differences between observations and simulations with more heavy precipitation  
266 events during regime HP in the observations while the simulations with CRCM5-LE show more precipitations  
267 events during regime South (Figure 5). The overestimation of the number of precipitation events for regime South  
268 can be associated to the difference in pattern between regimes calculated with 20thCR and CanESM2-LE (Figure  
269 3). Regime South calculated with CanESM2-LE shows Z500 anomalies shifted to the west and likely a more  
270 meridional flux compared to the regime South from 20thCR. The weather regimes associated to heavy  
271 precipitations in the Mid-west defined by Zhang and Villarini, (2019) show high pressure anomalies on the east  
272 and low pressure on the west sides of the Great lakes similarly to regime South calculated with CanESM2. The  
273 regime South calculated with 20thCR show negative Z500 anomalies with a northern position compared to  
274 CanESM2-LE and therefore a stronger zonal flux while the regime South calculated with CanESM2-LE has likely  
275 a more meridional flux driving humidity from the Gulf of Mexico (Figure 3). This pattern also brings warm  
276 temperature events even though the regime HP brings even more warm events in both the observations and the  
277 ensemble average (Figure 6). Regime HP has similarities with the positive phase of the NAO clearly associated  
278 with warm winter temperature in the Great Lakes region (Ning and Bradley, 2015). The other weather regimes  
279 bring generally fewer heavy precipitation or warm events apart from regime LP bringing heavy precipitation close  
280 to Lake Huron (Figure 5). LP is not associated with warm events (Figure 6) suggesting that these extreme  
281 precipitations are in form of snow and likely from lake effect snow. Suriano and Leathers, (2017) show that low  
282 pressure anomalies north-east from Great lakes brings major lake effects snow in the eastern shores of Lake Huron  
283 due to less zonal wind and cold outbreaks from the Arctic. The regime LP shows low geopotential height right on  
284 the Great lakes and the associated north-west winds on the Lake Huron are likely to bring lake effect snowfall in  
285 this area.

#### 286 **4.2 Future evolution of rain and warm events**

287 The future increase of heavy precipitations events in winter in Southern Ontario was already described in Deng *et*  
288 *al.*, (2016). Compound events such as Rain on Snow (ROS) events have also been investigated by Il Jeong and  
289 Sushama (2018). These authors defined ROS events as liquid precipitation and snow cover higher than 1mm and  
290 found no significant trend of ROS events in the Great lake region, in continuity to what was observed in the past  
291 (Wachowicz *et al.*, 2019). These studies show that the Great Lakes region is located between a region of increase  
292 ROS events due to increase of rainfall in the north and a decrease in ROS events due to decrease of snowpack in



293 southern regions. Increase of rainfall and decrease of snowpack are both likely to occur in Southern Ontario and  
294 are cancelling each other in term of ROS events. Our study does not consider snowpack and show an increase in  
295 heavy rain and warm compound events (Figure 9). The increase of heavy rain and warm events is likely driven  
296 by warmer temperature shown by the increase of the compound events and warm events both occurring at a higher  
297 extent close to Lake Erie (Figure 9). The increase in extreme precipitation events is less significant than the  
298 increase of warm events and is occurring mostly in the Northern parts of the area (Figure 9).

299

300 The future evolution of ROS or heavy rain and warm events corresponding to different weather patterns have not  
301 been yet investigated in previous literature. It is interesting to note that the future increase of the rain and warm  
302 events are expected to occur only for the regimes HP and South, the number of events remaining very low for the  
303 other regimes (Figure 9). This result suggests that the global increase of mean temperature and precipitation is not  
304 sufficient to reach the 10 mm and 5°C threshold for LP, North-West and North-East regimes. More precipitation  
305 events are expected during regimes LP but the temperature stays too low to increase the numbers of heavy rain  
306 and warm events (Figure 9). Regime North-West shows an increase of warm events but not an increase in  
307 precipitation events and therefore the number of rain and warm events is not expected to increase.

### 308 **4.3 Change in frequency of heavy rain and warm events partially modulated by the occurrence of weather** 309 **regimes**

310 Despite clear association between regimes HP/South and occurrences of rain and warm events, the uncertainties  
311 linked to internal variability of climate are not fully apprehended by the frequency of weather regimes. Members  
312 of the ensemble associated with a simultaneous high increase of regime HP and South frequencies are generally  
313 associated with higher increase in rainfall and warm events (Table 1) but the association is less straightforward  
314 than suggested by the correlation values (Figure 11) probably due to poor association between precipitation  
315 extremes and occurrence of weather regimes (Table 1 and Figure 10). Similar change in occurrences of South-HP  
316 weather regimes can lead to variable change in number of heavy rain and warm events (Figure 11). This suggests  
317 that other scales than the weather regimes calculated in the northeastern North American domain are likely to play  
318 a role in weather extreme events and especially the change of heavy rain and warm events and precipitation events.  
319 The presence of the Great lakes has a large role in the variability of precipitation at a local scale (Martynov et al.,  
320 2012) suggesting that variability of precipitation events depend not so much on the atmospheric circulation over  
321 the Great Lakes at the day of the events. The temperature of the lakes and the amount of ice covering the lakes  
322 plays a great role in the variability of precipitation (Martynov et al., 2012).



#### 323 4.4 Non stationarity in the relationship between weather extreme events and high flows

324 The projections show that the increase in number of high flows associated to a regime HP is expected to be lower  
325 than the increase in number of heavy rain and warm events (negative DIF in Figure 10). This result suggests that  
326 the conditions to produce high flows may change in the future. As the temperature increase, snowmelt is expected  
327 to be a less important component in the generation of high flows in the region. In the historical period regimes HP  
328 and South produce approximately the same number of high flows in the simulations (Figure 7) but are driving  
329 mostly by heavy precipitation for the regime South and warm events for the regime HP (Figure 5 and 6). More  
330 importantly, HP shows a further increase of warm events in the future while South show rather an increase of  
331 precipitation (Figure 9). In the context of less snow, the importance of precipitation to drive high flows will be  
332 higher in the future because warmer conditions do not increase snowmelt in case of a snowpack reduction.  
333 Therefore, the increase of weather extreme events associated to the regime South will be associated to an increase  
334 of high flows more strenuously than the increase of events associated to HP.

335 The future change in number of high flows is associate to a large inter-member uncertainty (Figure 10). The  
336 weather extreme events inter-member uncertainty was partly associated to the change in occurrence of weather  
337 regimes especially for the warm component (Figure 11 and 12 and Table 1). The association between occurrence  
338 of weather regimes and high flows is less clear and shows opposite results (Table 1 and 2). Especially, change of  
339 occurrence of regime North-west is positively correlated to the change in number of high flows in Big Creek  
340 watershed (Table 2) while it is negatively correlated to the change in number of weather extreme events in this  
341 area (Figure 11). The correlation is also significant when regimes North-west and South are associated (Table 2).  
342 This result can be due to the continuous nature of streamflow and the preferential sequence of weather regimes.  
343 Regime North-west shows an increase in number of warm events especially close to Lake Erie (Figure 9) with the  
344 potentiality to melt more snow in the future. The amount of precipitation generated by a regime North-west is  
345 probably not sufficient to generate high flows (Figure 9), but the increase of snowmelt during the regime North-  
346 West likely enhances streamflow that make the high flows threshold easier to reach in a following precipitation  
347 event. The pattern associated with regime North-west shows anticyclonic systems in the west part of the domain  
348 (Figure 3). The meteorological systems have a tendency to move eastward and this anticyclonic system is likely  
349 to become a regime South or HP (Champagne *et al.*, 2019, Supplementary material, Table S2). As already stated  
350 in the previous paragraph, regime HP will be less likely to produce a heavy rain event than a regime South in the  
351 future. The combination of the warmer regime North-west following by a wetter and warmer regime South are  
352 therefore more likely to produce high flows in the future. These results emphasize the need to study not only each



353 hydrometeorological extreme events and relationship with atmospheric circulation independently, but also  
354 focusing on the sequence of weather patterns preceding the high flows events.

#### 355 **4.5 Relevance of rain and warm events to explain future evolution of high flows**

356 One of the objectives of this study was mainly to create a new index that explains high flows in Southern Ontario  
357 and investigate how this index will change in the near future. However, as stated in the previous section, the  
358 relationship between the extreme weather events index and high flows is affected by non-stationarity. Applied in  
359 the past, the Rain and warm index works well to define the high flows risk in Southern Ontario (Figure 2), the  
360 warm component of this index being a condition to trigger snowmelt. In a warming climate, snowpack is reduced,  
361 and the rain to snow ratio is increasing (Il Jeong and Sushama, 2018), changing the relationship between extreme  
362 weather events and high flows. Rain on snow index could be used in lieu of our heavy rain and warm index but  
363 this index is not projected to be more frequent in the future in the Great Lakes region, precisely because of less  
364 snow in the ground (Il Jeong and Sushama, 2018). Moreover, ROS index integrate events with a very small  
365 contribution of snowmelt to the high flows while neglecting rainfall only events (Cohen et al., 2015; Il Jeong and  
366 Sushama, 2018; Pradhanang et al., 2013). The definition of ROS also introduces more uncertainties as it depends  
367 on the combination of simulated precipitation and temperature for several days (Kudo et al., 2017). Our heavy  
368 rain and warm index minimizes this uncertainty and take into consideration heavy rainfall whatever the amount  
369 of snow covering the ground. It is therefore a good tool to assess the potential risk of high flows in Southern  
370 Ontario from all ranges of rain events, even though it is important to keep in mind that the flood risk diminished  
371 as snowpack decreases. A rain only index could also be used but the impact of snowpack on streamflow would be  
372 completely eradicated while snow will still play a role in the future hydrology. ROS events, liquid precipitation  
373 events and our heavy rain and warm events should be investigated together to fully understand the future evolution  
374 of the flood risk due to a shift in weather extreme events.

#### 375 **5 Conclusion**

376 The aim of this study was to assess the ability of the Canadian Regional Climate Model Large Ensemble (CRCM5-  
377 LE), a downscaled version of the 50-members global Canadian model Large Ensemble (CanESM2-LE), to  
378 simulate winter hydrometeorological extreme events in Southern Ontario and to investigate how the internal  
379 variability of climate will modulate the future evolution of these extremes. The winter composite index heavy rain  
380 and warm temperature was identified in the past with gridded observation data (CanGRD) by investigating what



381 conditions of temperature and precipitation are necessary to produce a high flow in three watersheds in Southern  
382 Ontario. PRMS model was used to simulate the future evolution of high flows for each member of CRCM-LE in  
383 these three watersheds. The large-scale circulation patterns corresponding to these events were assessed by  
384 identifying past recurrent weather regimes based on daily Z500 from the 20th century reanalyses and estimating  
385 the evolution of the same weather regimes in the future for each member of CanESM2-LE. The results of this  
386 study show that CRCM5-LE was able to:

- 387 (1) Recreate the historical larger number of events close to Lake Erie despite an overestimation of warm  
388 events.
- 389 (2) Simulate more heavy rain and warm events as well as high flows during the regimes associated with high  
390 pressure anomalies on the Great Lakes (HP) and the Atlantic-Ocean (South).
- 391 (3) Project an increase in the future number of heavy rain and warm events and associated high flows  
392 especially during the regimes HP and South and in the vicinity of Lake Erie.

393 These results suggest that depending on the future evolution of natural variability of climate, the increase in the  
394 number of events will be amplified or attenuated by the favoured positions of the pressure systems. The natural  
395 variability of climate is not expected to greatly modulate the number of high flows due to an increase of the  
396 importance of precipitation in generating high flows. The role of more localized processes such as impact of the  
397 lakes on precipitation events needs to be further evaluated to improve the ability of the next versions of regional  
398 climate models to recreate the precipitation events. The newly created weather index did not integrate snowpack  
399 because the uncertainties in the ability of CRCM5-LE to recreate precipitation and temperature extremes at a daily  
400 basis would be further increase in snowmelt estimates. However, snowpack variability will have a large impact in  
401 the modulation of high flows in the region and future studies should investigate snow processes by taking  
402 advantage of rapid improvements in climate regional modelling. Other regional climate models and different  
403 scenarios should also be used to improve our understanding in the future evolution of hydrometeorological  
404 extreme events in Southern Ontario. Despite these future possible improvements, our study gives a good  
405 estimation of what to expect in term of change in number of hydrometeorological events in Southern Ontario and  
406 will serve to better estimate the future flood risk in this populated region.

#### 407 **Authors contribution**

408 ML furnished CRCM5-LE data. OC performed the analyses and made the figures. OC prepared the manuscript  
409 with contributions from all co-authors.



#### 410 **Competing interest**

411 The authors declare that they have no conflict of interest.

#### 412 **Acknowledgement**

413 Financial support for this study was provided by the Natural Sciences and Engineering Research Council  
414 (NSERC) of Canada through the FloodNet Project. We also acknowledge support and contributions from Global  
415 Water Future Program, Environment and Climate Change Canada, Natural Resources Canada and Water Survey  
416 of Canada. The production of ClimEx was funded within the ClimEx project by the Bavarian State Ministry for  
417 the Environment and Consumer Protection. The CRCM5 was developed by the ESCER centre of Université du  
418 Québec à Montréal (UQAM; [www.escer.uqam.ca](http://www.escer.uqam.ca)) in collaboration with Environment and Climate Change  
419 Canada. We acknowledge Environment and Climate Change Canada's Canadian Centre for Climate Modelling  
420 and Analysis for executing and making available the CanESM2 Large Ensemble simulations used in this study,  
421 and the Canadian Sea Ice and Snow Evolution Network for proposing the simulations. Computations with the  
422 CRCM5 for the ClimEx project were made on the SuperMUC supercomputer at Leibniz Supercomputing Centre  
423 (LRZ) of the Bavarian Academy of Sciences and Humanities. The operation of this supercomputer is funded via  
424 the Gauss Centre for Supercomputing (GCS) by the German Federal Ministry of Education and Research and the  
425 Bavarian State Ministry of Education, Science and the Arts.

#### 426 **References**

427 Buttle, J. M., Allen, D. M., Caissie, D., Davison, B., Hayashi, M., Peters, D. L., Pomeroy, J. W., Simonovic, S.,  
428 St-Hilaire, A. and Whitfield, P. H.: Flood processes in Canada: Regional and special aspects, *Canadian Water*  
429 *Resources Journal / Revue canadienne des ressources hydriques*, 1–24, doi:10.1080/07011784.2015.1131629,  
430 2016.

431 Champagne, O., Arain, M. A. and Coulibaly, P.: Atmospheric circulation amplifies shift of winter streamflow in  
432 Southern Ontario, *Journal of Hydrology*, 124051, doi:10.1016/j.jhydrol.2019.124051, 2019.

433 Cohen, J., Ye, H. and Jones, J.: Trends and variability in rain-on-snow events: RAIN-ON-SNOW, *Geophysical*  
434 *Research Letters*, 42(17), 7115–7122, doi:10.1002/2015GL065320, 2015.

435 Compo, G. P., Whitaker, J. S., Sardeshmukh, P. D., Matsui, N., Allan, R. J., Yin, X., Gleason, B. E., Vose, R. S.,  
436 Rutledge, G., Bessemoulin, P. and others: The twentieth century reanalysis project, *Quarterly Journal of the Royal*  
437 *Meteorological Society*, 137(654), 1–28, doi:10.1002/qj.776, 2011.





- 438 Deng, Z., Qiu, X., Liu, J., Madras, N., Wang, X. and Zhu, H.: Trend in frequency of extreme precipitation events  
439 over Ontario from ensembles of multiple GCMs, *Climate Dynamics*, 46(9–10), 2909–2921, doi:10.1007/s00382-  
440 015-2740-9, 2016.
- 441 Deser, C., Phillips, A. S., Alexander, M. A. and Smoliak, B. V.: Projecting North American climate over the next  
442 50 years: uncertainty due to internal variability\*, *Journal of Climate*, 27(6), 2271–2296, 2014.
- 443 Dressler, K. A., Leavesley, G. H., Bales, R. C. and Fassnacht, S. R.: Evaluation of gridded snow water equivalent  
444 and satellite snow cover products for mountain basins in a hydrologic model, *Hydrological Processes*, 20(4), 673–  
445 688, doi:10.1002/hyp.6130, 2006.
- 446 Farnham, D. J., Doss-Gollin, J. and Lall, U.: Regional Extreme Precipitation Events: Robust Inference From  
447 Credibly Simulated GCM Variables, *Water Resources Research*, 54(6), 3809–3824,  
448 doi:10.1002/2017WR021318, 2018.
- 449 Freudiger, D., Kohn, I., Stahl, K. and Weiler, M.: Large-scale analysis of changing frequencies of rain-on-snow  
450 events with flood-generation potential, *Hydrology and Earth System Sciences*, 18(7), 2695–2709,  
451 doi:10.5194/hess-18-2695-2014, 2014.
- 452 Hoegh-Guldberg, O., Jacob, D., Taylor, M., Bindi, M., Brown, S., Camilloni, I., Diedhiou, A., Djalante, R., Ebi,  
453 K. L., Engelbrecht, F., Guiot, J., Hijioka, Y., Mehrotra, S., Seneviratne, S. I., Thomas, A., Warren, R., Halim, S.  
454 A., Achlatis, M., Alexander, L. V., Berry, P., Boyer, C., Byers, E., Brilli, L., Buckeridge, M., Cheung, W., Craig,  
455 M., Evans, J., Fischer, H., Fraedrich, K., Ganase, A., Gattuso, J. P., Bolaños, T. G., Hanasaki, N., Hayes, K.,  
456 Hirsch, A., Jones, C., Jung, T., Kanninen, M., Krinner, G., Lawrence, D., Ley, D., Liverman, D., Mahowald, N.,  
457 Meissner, K. J., Millar, R., Mintenbeck, K., Mix, A. C., Notz, D., Nurse, L., Okem, A., Olsson, L., Oppenheimer,  
458 M., Paz, S., Petersen, J., Petzold, J., Preuschmann, S., Rahman, M. F., Scheuffele, H., Schleussner, C.-F., Séférian,  
459 R., Sillmann, J., Singh, C., Slade, R., Stephenson, K., Stephenson, T., Tebboth, M., Tschakert, P., Vautard, R.,  
460 Wehner, M., Weyer, N. M., Whyte, F., Yohe, G., Zhang, X., Zougmore, R. B., Marengo, J. A., Pereira, J. and  
461 Sherstyukov, B.: Impacts of 1.5°C of Global Warming on Natural and Human Systems, , 138, 2018.
- 462 Il Jeong, D. and Sushama, L.: Rain-on-snow events over North America based on two Canadian regional climate  
463 models, *Climate Dynamics*, 50(1–2), 303–316, doi:10.1007/s00382-017-3609-x, 2018.
- 464 Ines, A. V. M. and Hansen, J. W.: Bias correction of daily GCM rainfall for crop simulation studies, *Agricultural  
465 and Forest Meteorology*, 138(1–4), 44–53, doi:10.1016/j.agrformet.2006.03.009, 2006.
- 466 Kharin, V. V., Zwiers, F. W., Zhang, X. and Wehner, M.: Changes in temperature and precipitation extremes in  
467 the CMIP5 ensemble, *Climatic Change*, 119(2), 345–357, doi:10.1007/s10584-013-0705-8, 2013.
- 468 Kudo, R., Yoshida, T. and Masumoto, T.: Uncertainty analysis of impacts of climate change on snow processes:  
469 Case study of interactions of GCM uncertainty and an impact model, *Journal of Hydrology*, 548, 196–207,  
470 doi:10.1016/j.jhydrol.2017.03.007, 2017.
- 471 Lafaysse, M., Hingray, B., Mezghani, A., Gailhard, J. and Terray, L.: Internal variability and model uncertainty  
472 components in future hydrometeorological projections: The Alpine Durance basin, *Water Resources Research*,  
473 50(4), 3317–3341, doi:10.1002/2013WR014897, 2014.



- 474 Leduc, M., Mailhot, A., Frigon, A., Martel, J.-L., Ludwig, R., Brietzke, G. B., Giguère, M., Brissette, F., Turcotte,  
475 R., Braun, M. and Scinocca, J.: The ClimEx Project: A 50-Member Ensemble of Climate Change Projections at  
476 12-km Resolution over Europe and Northeastern North America with the Canadian Regional Climate Model  
477 (CRCM5), *Journal of Applied Meteorology and Climatology*, 58(4), 663–693, doi:10.1175/JAMC-D-18-0021.1,  
478 2019.
- 479 Leonard, M., Westra, S., Phatak, A., Lambert, M., van den Hurk, B., McInnes, K., Risbey, J., Schuster, S., Jakob,  
480 D. and Stafford-Smith, M.: A compound event framework for understanding extreme impacts: A compound event  
481 framework, *Wiley Interdisciplinary Reviews: Climate Change*, 5(1), 113–128, doi:10.1002/wcc.252, 2014.
- 482 Liao, C. and Zhuang, Q.: Quantifying the Role of Snowmelt in Stream Discharge in an Alaskan Watershed: An  
483 Analysis Using a Spatially Distributed Surface Hydrology Model: ROLE OF SNOWMELT IN STREAMFLOW  
484 IN ALASKA, *Journal of Geophysical Research: Earth Surface*, 122(11), 2183–2195, doi:10.1002/2017JF004214,  
485 2017.
- 486 Lorenz, E. N.: Deterministic Nonperiodic Flow, *Journal of the Atmospheric Sciences*, 20(2), 130–141,  
487 doi:10.1175/1520-0469(1963)020<0130:DNF>2.0.CO;2, 1963.
- 488 Mallakpour, I. and Villarini, G.: Investigating the relationship between the frequency of flooding over the central  
489 United States and large-scale climate, *Advances in Water Resources*, 92, 159–171,  
490 doi:10.1016/j.advwatres.2016.04.008, 2016.
- 491 Markstrom, S. L., Regan, R. S., Hay, L. E., Viger, R. J., Payn, R. A. and LaFontaine, J. H.: precipitation-runoff  
492 modeling system, version 4: U.S. Geological Survey Techniques and Methods., 2015.
- 493 Martynov, A., Sushama, L., Laprise, R., Winger, K. and Dugas, B.: Interactive lakes in the Canadian Regional  
494 Climate Model, version 5: the role of lakes in the regional climate of North America, *Tellus A: Dynamic  
495 Meteorology and Oceanography*, 64(1), 16226, doi:10.3402/tellusa.v64i0.16226, 2012.
- 496 Mastin, M. C., Chase, K. J. and Dudley, R. W.: Changes in Spring Snowpack for Selected Basins in the United  
497 States for Different Climate-Change Scenarios, *Earth Interactions*, 15(23), 1–18, doi:10.1175/2010EI368.1, 2011.
- 498 McCabe, G. J., Clark, M. P. and Hay, L. E.: Rain-on-Snow Events in the Western United States, *Bulletin of the  
499 American Meteorological Society*, 88(3), 319–328, doi:10.1175/BAMS-88-3-319, 2007.
- 500 McKenney, D. W., Hutchinson, M. F., Papadopol, P., Lawrence, K., Pedlar, J., Campbell, K., Milewska, E.,  
501 Hopkinson, R. F., Price, D. and Owen, T.: Customized Spatial Climate Models for North America, *Bulletin of the  
502 American Meteorological Society*, 92(12), 1611–1622, doi:10.1175/2011BAMS3132.1, 2011.
- 503 Merz, R. and Blöschl, G.: A process typology of regional floods: PROCESS TYPOLOGY OF REGIONAL  
504 FLOODS, *Water Resources Research*, 39(12), doi:10.1029/2002WR001952, 2003.
- 505 Michelangeli, P.-A., Vautard, R. and Legras, B.: Weather Regimes: Recurrence and Quasi Stationarity, *Journal  
506 of the Atmospheric Sciences*, 52(8), 1237–1256, doi:10.1175/1520-0469(1995)052<1237:WRRRAQS>2.0.CO;2,  
507 1995.



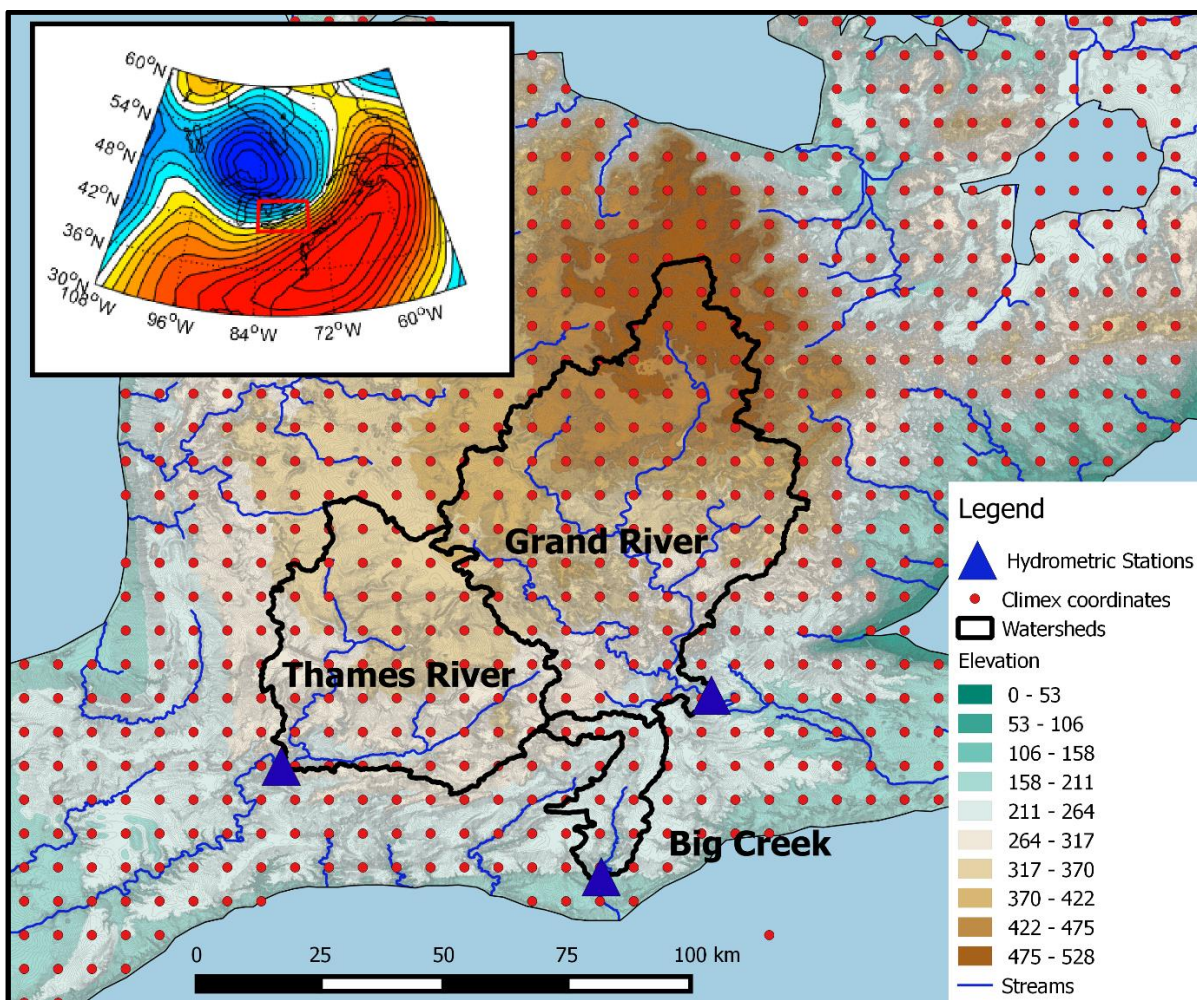
- 508 Musselman, K. N., Lehner, F., Ikeda, K., Clark, M. P., Prein, A. F., Liu, C., Barlage, M. and Rasmussen, R.:  
509 Projected increases and shifts in rain-on-snow flood risk over western North America, *Nature Climate Change*,  
510 8(9), 808–812, doi:10.1038/s41558-018-0236-4, 2018.
- 511 Ning, L. and Bradley, R. S.: Winter climate extremes over the northeastern United States and southeastern Canada  
512 and teleconnections with large-scale modes of climate variability\*, *Journal of Climate*, 28(6), 2475–2493, 2015.
- 513 Pradhanang, S. M., Frei, A., Zion, M., Schneiderman, E. M., Steenhuis, T. S. and Pierson, D.: Rain-on-snow  
514 runoff events in New York: RAIN-ON-SNOW EVENTS IN NEW YORK, *Hydrological Processes*, 27(21), 3035–  
515 3049, doi:10.1002/hyp.9864, 2013.
- 516 Scott, R. W. and Huff, F. A.: Impacts of the Great Lakes on regional climate conditions, *Journal of Great Lakes  
517 Research*, 22(4), 845–863, 1996.
- 518 Surfleet, C. G. and Tullos, D.: Variability in effect of climate change on rain-on-snow peak flow events in a  
519 temperate climate, *Journal of Hydrology*, 479, 24–34, doi:10.1016/j.jhydrol.2012.11.021, 2013.
- 520 Surfleet, C. G., Tullos, D., Chang, H. and Jung, I.-W.: Selection of hydrologic modeling approaches for climate  
521 change assessment: A comparison of model scale and structures, *Journal of Hydrology*, 464–465, 233–248,  
522 doi:10.1016/j.jhydrol.2012.07.012, 2012.
- 523 Suriano, Z. J. and Leathers, D. J.: Synoptic climatology of lake-effect snowfall conditions in the eastern Great  
524 Lakes region: SYNOPTIC CLIMATOLOGY OF LAKE-EFFECT SNOWFALL CONDITIONS, *International  
525 Journal of Climatology*, 37(12), 4377–4389, doi:10.1002/joc.5093, 2017.
- 526 Teng, F., Huang, W., Cai, Y., Zheng, C. and Zou, S.: Application of Hydrological Model PRMS to Simulate Daily  
527 Rainfall Runoff in Zamask-Yingluoxia Subbasin of the Heihe River Basin, *Water*, 9(10), 769,  
528 doi:10.3390/w9100769, 2017.
- 529 Teng, F., Huang, W. and Ginis, I.: Hydrological modeling of storm runoff and snowmelt in Taunton River Basin  
530 by applications of HEC-HMS and PRMS models, *Natural Hazards*, 91(1), 179–199, doi:10.1007/s11069-017-  
531 3121-y, 2018.
- 532 Thiombiano, A. N., El Adlouni, S., St-Hilaire, A., Ouarda, T. B. M. J. and El-Jabi, N.: Nonstationary frequency  
533 analysis of extreme daily precipitation amounts in Southeastern Canada using a peaks-over-threshold approach,  
534 *Theoretical and Applied Climatology*, 129(1–2), 413–426, doi:10.1007/s00704-016-1789-7, 2017.
- 535 Trenberth, K. E.: Conceptual Framework for Changes of Extremes of the Hydrological Cycle with Climate  
536 Change, *Climatic Change*, 42(1), 327–339, doi:10.1023/A:1005488920935, 1999.
- 537 Wachowicz, L. J., Mote, T. L. and Henderson, G. R.: A rain on snow climatology and temporal analysis for the  
538 eastern United States, *Physical Geography*, 1–16, doi:10.1080/02723646.2019.1629796, 2019.
- 539 Würzer, S., Jonas, T., Wever, N. and Lehning, M.: Influence of Initial Snowpack Properties on Runoff Formation  
540 during Rain-on-Snow Events, *Journal of Hydrometeorology*, 17(6), 1801–1815, doi:10.1175/JHM-D-15-0181.1,  
541 2016.



- 542 Zhang, W. and Villarini, G.: On the weather types that shape the precipitation patterns across the U.S. Midwest,  
543 Climate Dynamics, doi:10.1007/s00382-019-04783-4, 2019.
- 544 Zhang, X., Alexander, L., Hegerl, G. C., Jones, P., Tank, A. K., Peterson, T. C., Trewin, B. and Zwiers, F. W.:  
545 Indices for monitoring changes in extremes based on daily temperature and precipitation data, Wiley  
546 Interdisciplinary Reviews: Climate Change, 2(6), 851–870, doi:10.1002/wcc.147, 2011.
- 547 Zhao, H., Higuchi, K., Waller, J., Auld, H. and Mote, T.: The impacts of the PNA and NAO on annual maximum  
548 snowpack over southern Canada during 1979-2009, International Journal of Climatology, 33(2), 388–395,  
549 doi:10.1002/joc.3431, 2013.



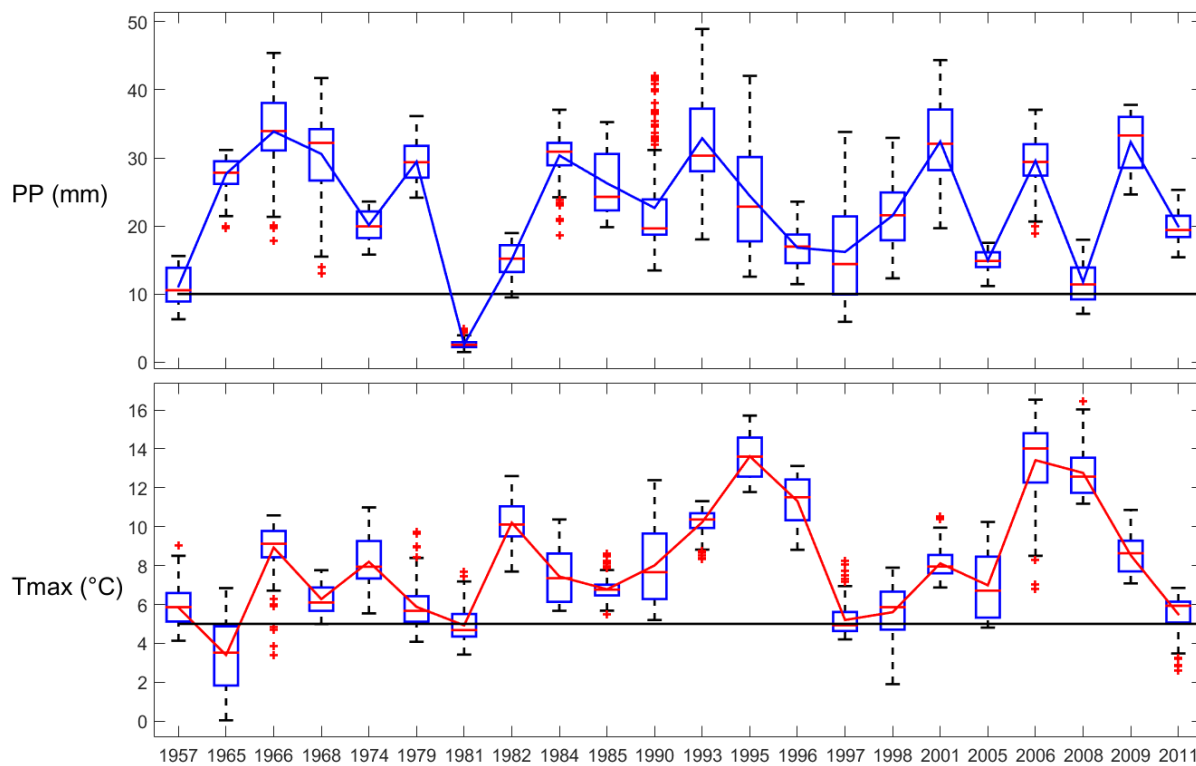
550



551

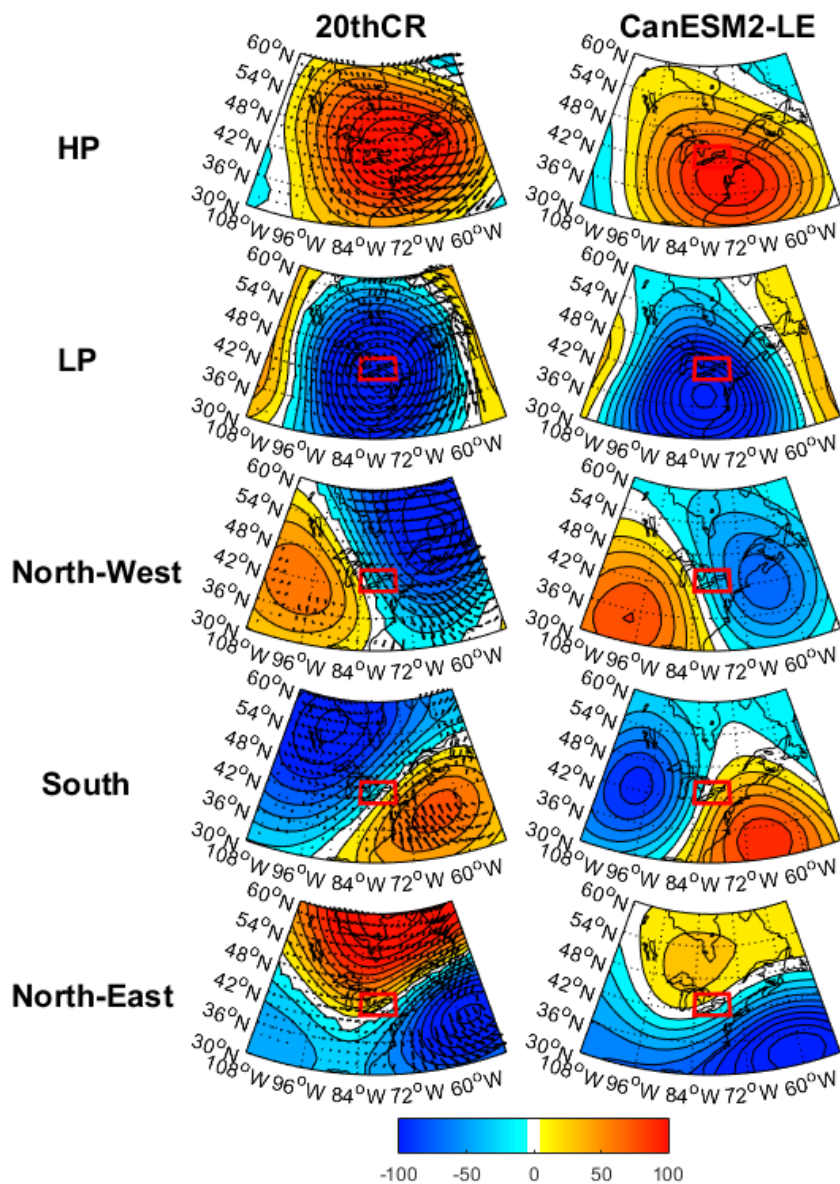
552 Figure 1: Location of the three watersheds and the ClimEx grid points used in this study and situation in the  
553 northeastern North America domain (Inset)





554

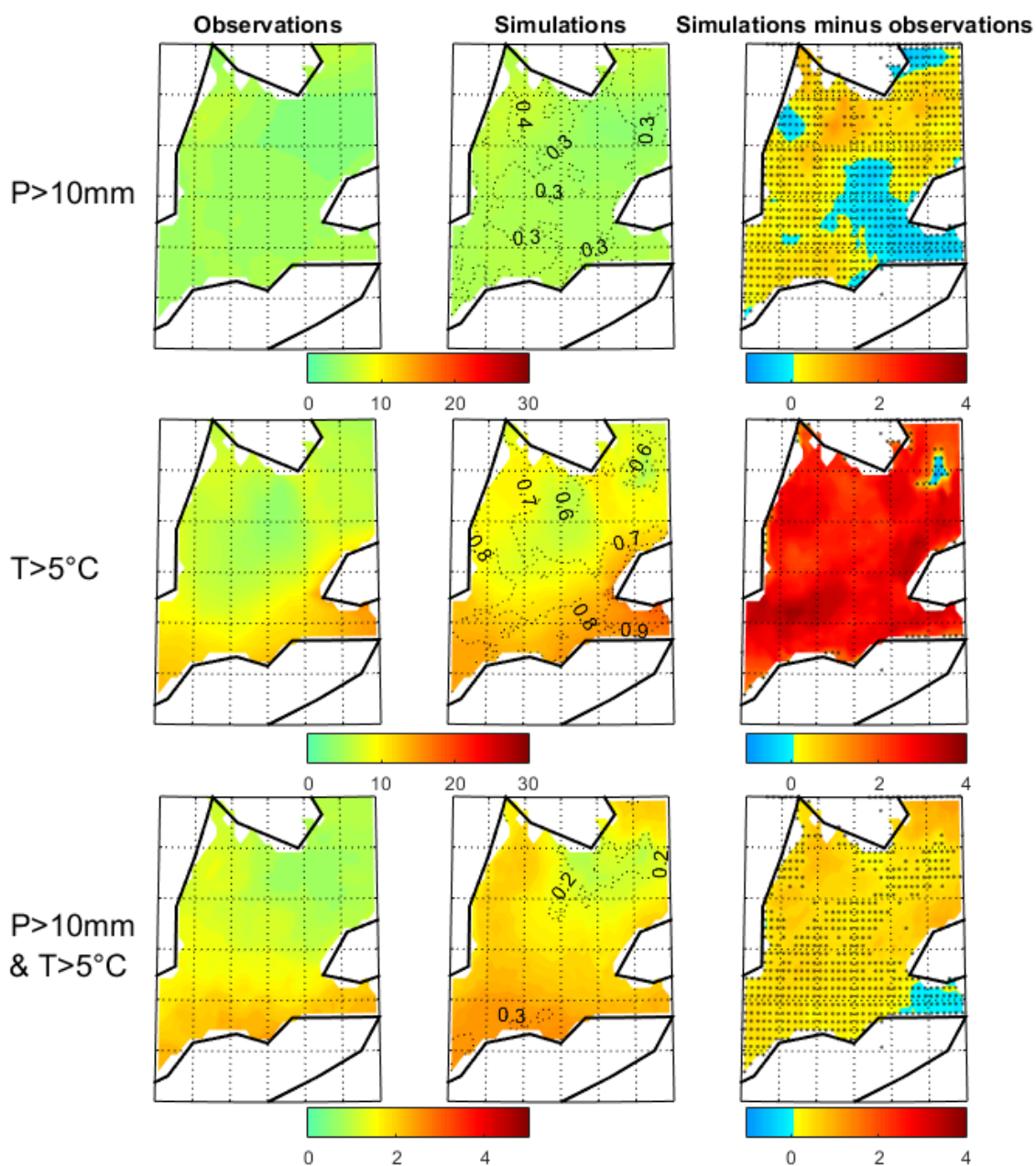
555 **Figure 2: Distribution of CanGRD temperature and precipitation from all 3 watersheds grid-points corresponding to**  
556 **each DJF high-flow event. Boxes extend from the 25th to the 75th percentile, with a horizontal red bar showing the**  
557 **median value. The whiskers are lines extending from each end of the box to the 1.5 interquartile range. Plus signs**  
558 **correspond to outliers. The blue lines correspond to high flows (Average streamflow plus 3 times the standard**  
559 **deviation). The horizontal black lines correspond to the thresholds used to define DJF extreme events.**



560

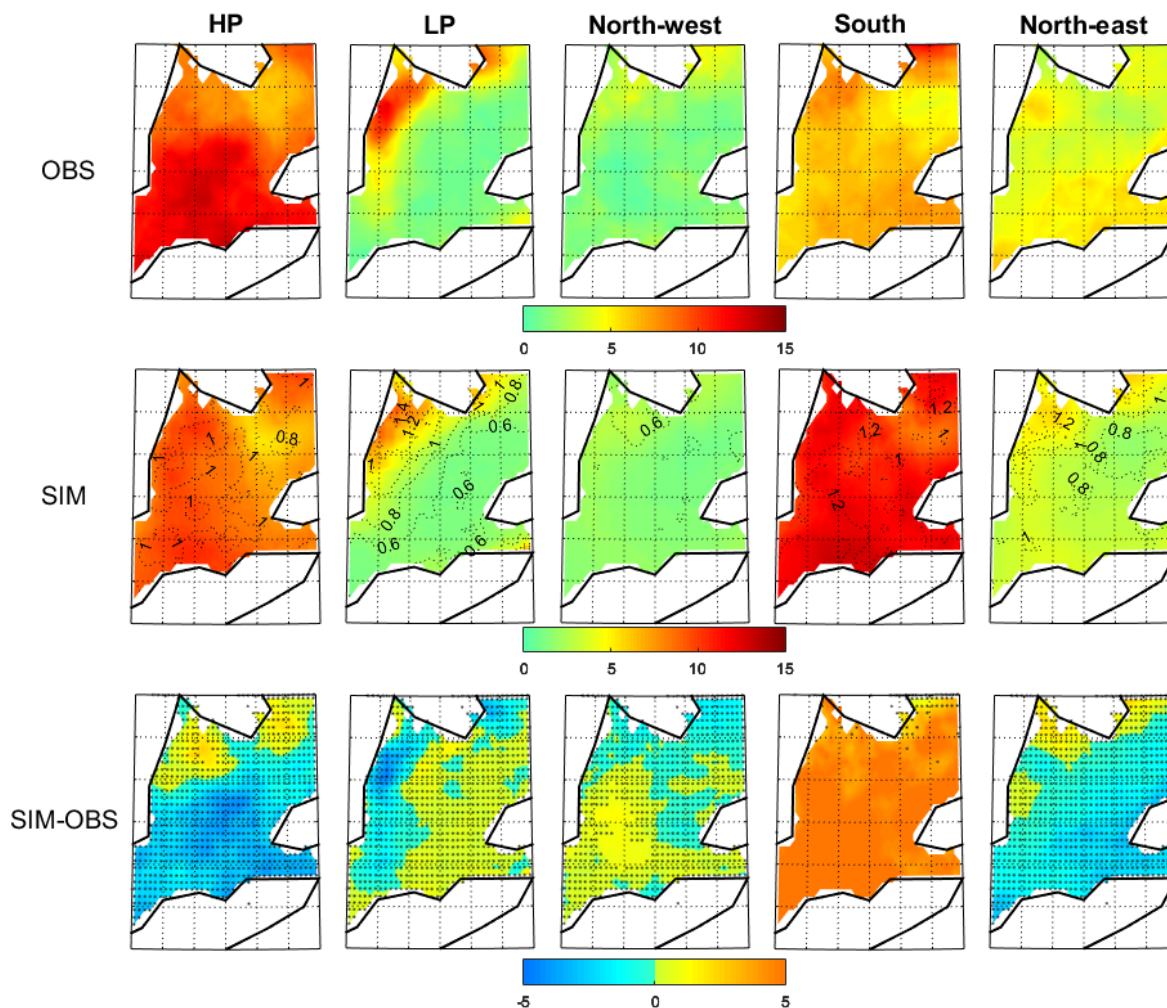
561 **Figure 3:** Left: DJF Z500 anomalies (colours) and winds (vectors) corresponding to Weather regimes calculated with  
562 20thCR. Right: DJF 50 members average Z500 anomalies calculated with CanESM2-LE.





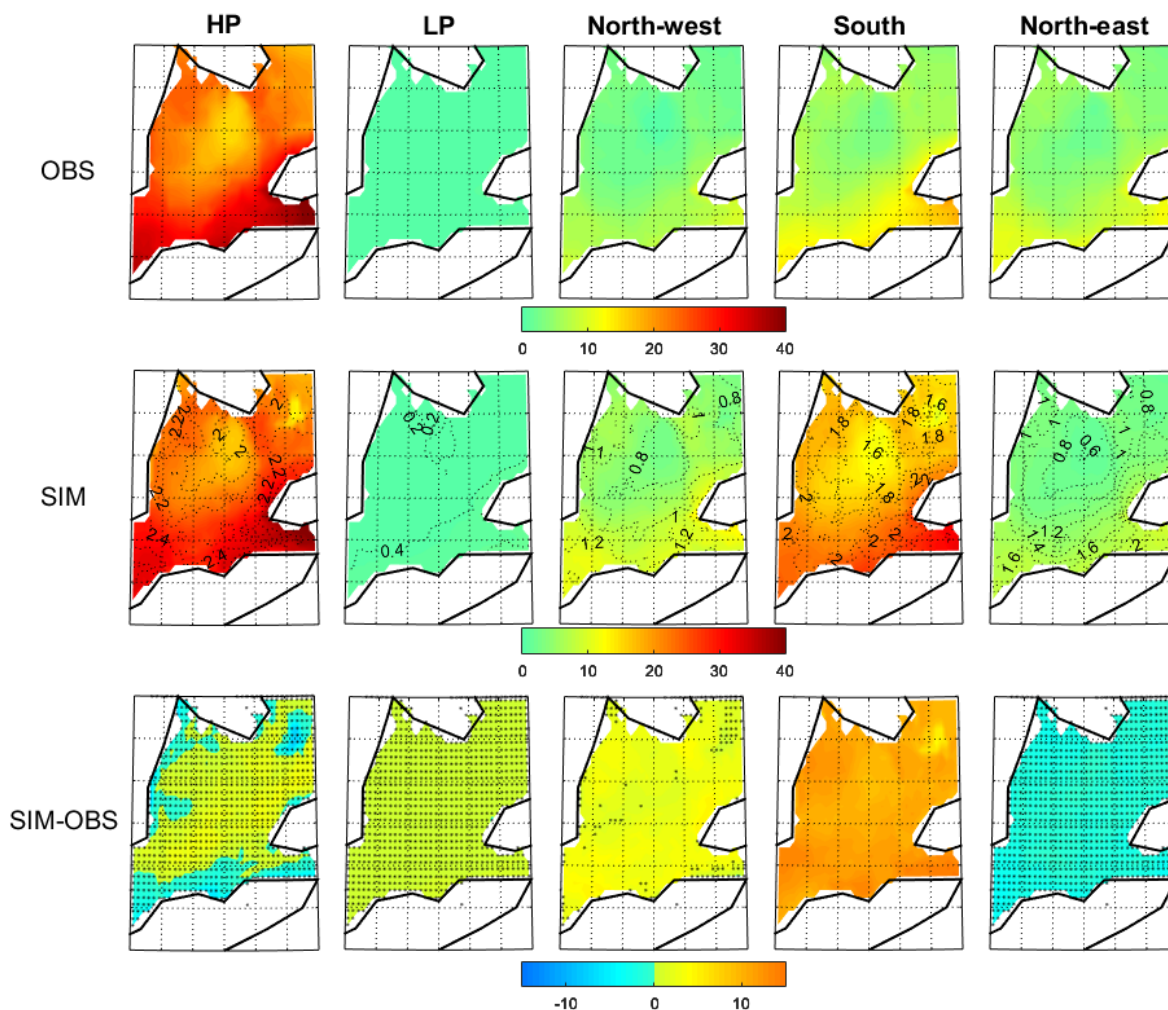
563

564 **Figure 4: DJF number of precipitation and warm extreme events in the historical period (1961-1990) for CanGRD (left**  
 565 **panels), 50 members CRCM5-LE average (mid panels) and CanGRD minus CRCM5-LE (right panels). The dotted**  
 566 **lines in the mid panels represent the standard deviation of the 50-members CRCM5-LE simulated number of events.**  
 567 **Stippled regions in the right panels indicate where the observations lie within the CRCM5-LE ensemble spread.**



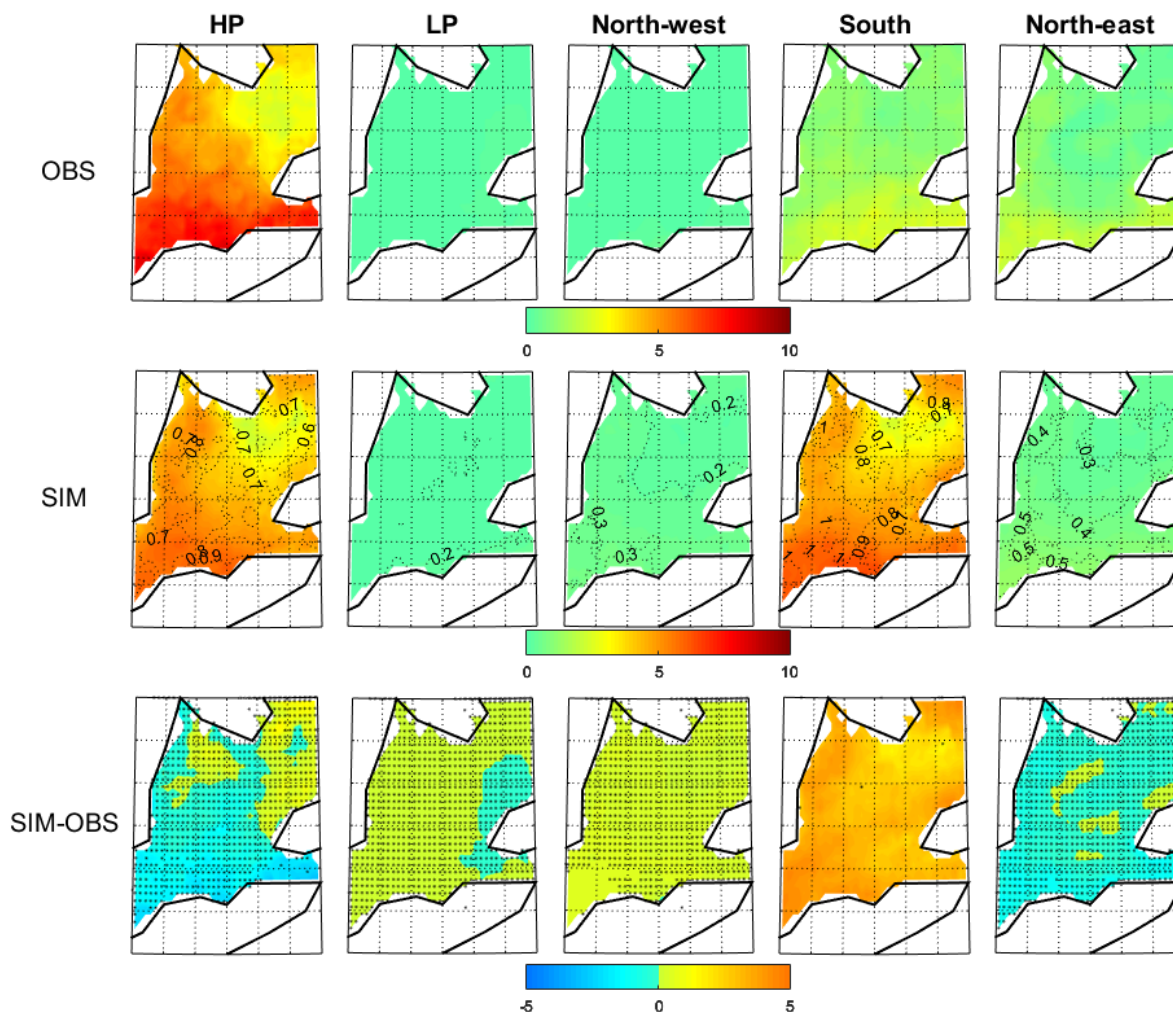
568

569 **Figure 5: Percentage of DJF number of precipitation events relative to DJF occurrence of weather regimes in the**  
 570 **historical period (1961-1990) for CanGRD (upper panels), 50 members CRCM5-LE average (mid panels) and CanGRD**  
 571 **minus CRCM5-LE (right panels). The dotted lines in the mid panels represent the standard deviation of the 50-**  
 572 **members CRCM5-LE simulated percentage. Stippled regions in the lower panels indicate where the observations lie**  
 573 **within the CRCM5-LE ensemble spread.**



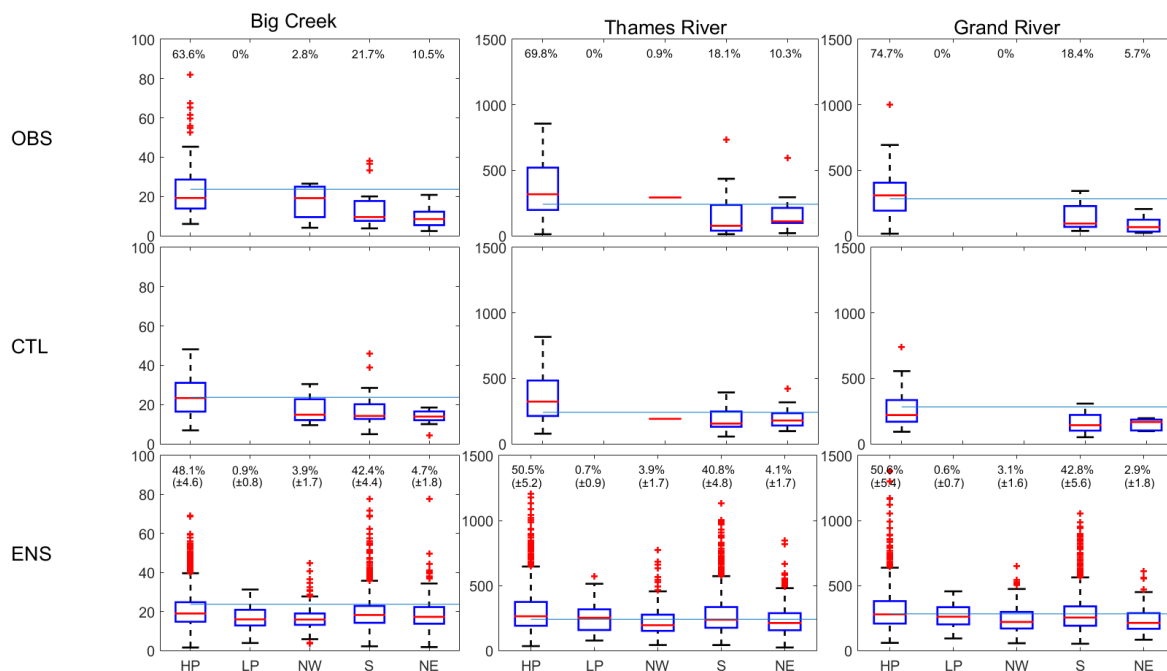
574

575 **Figure 6: Percentage of DJF number of warm events relative to DJF occurrence of weather regime in the historical**  
 576 **period (1961-1990) for CanGRD (upper panels), 50 members CRCM5-LE average (mid panels) and CanGRD minus**  
 577 **CRCM5-LE (lower panels). The dotted lines in the mid panels represent the standard deviation of the 50-members**  
 578 **CRCM5-LE simulated percentage. Stippled regions in the lower panels indicate where the observations lie within the**  
 579 **CRCM5-LE ensemble spread.**



580

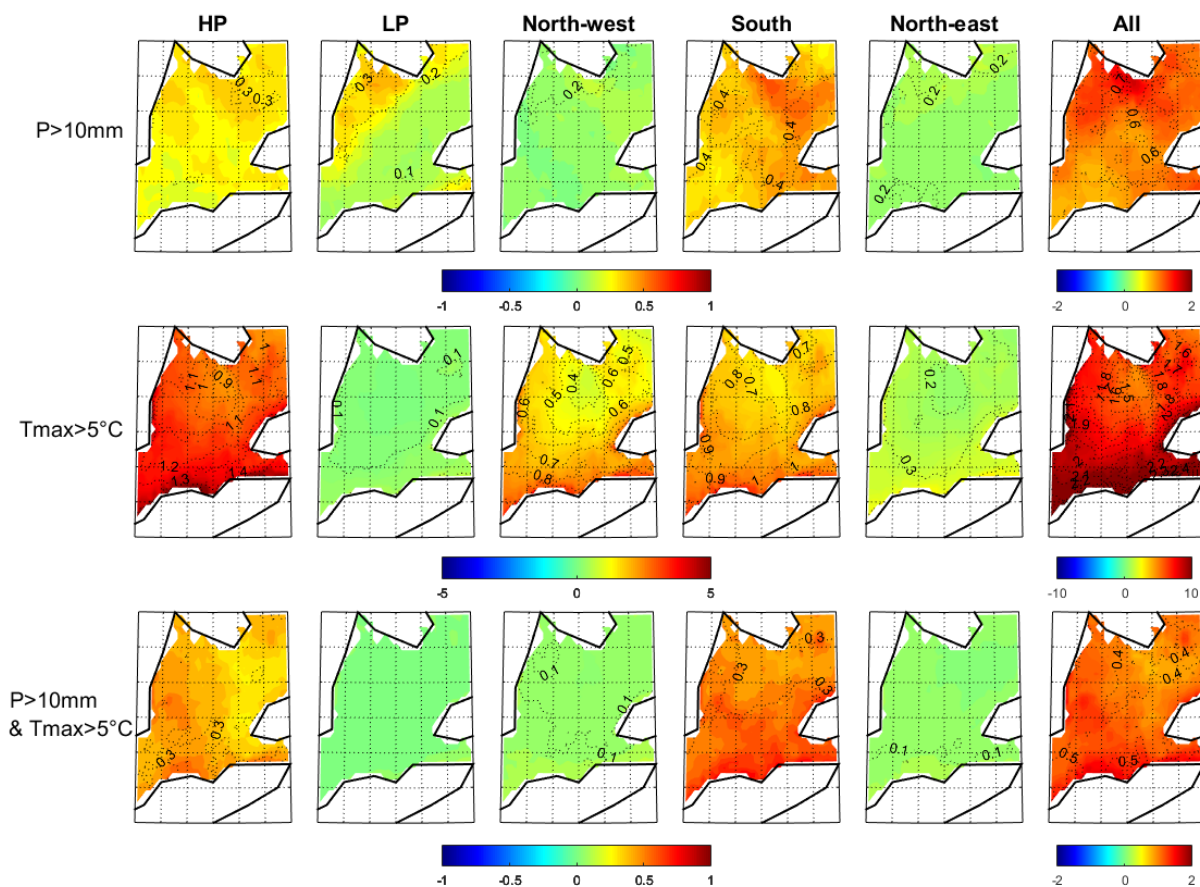
581 **Figure 7: Percentage of DJF number of heavy rain and warm events relative to DJF occurrence of weather regimes in**  
 582 **the historical period (1961-1990) for CanGRD (upper panels), 50 members CRCM5-LE average (mid panels) and**  
 583 **CanGRD minus CRCM5-LE (lower panels). The dotted lines in the mid panels represent the standard deviation of the**  
 584 **50-members CRCM5-LE simulated percentage. Stippled regions in the lower panels indicate where the observations**  
 585 **lie within the CRCM5-LE ensemble spread.**



586

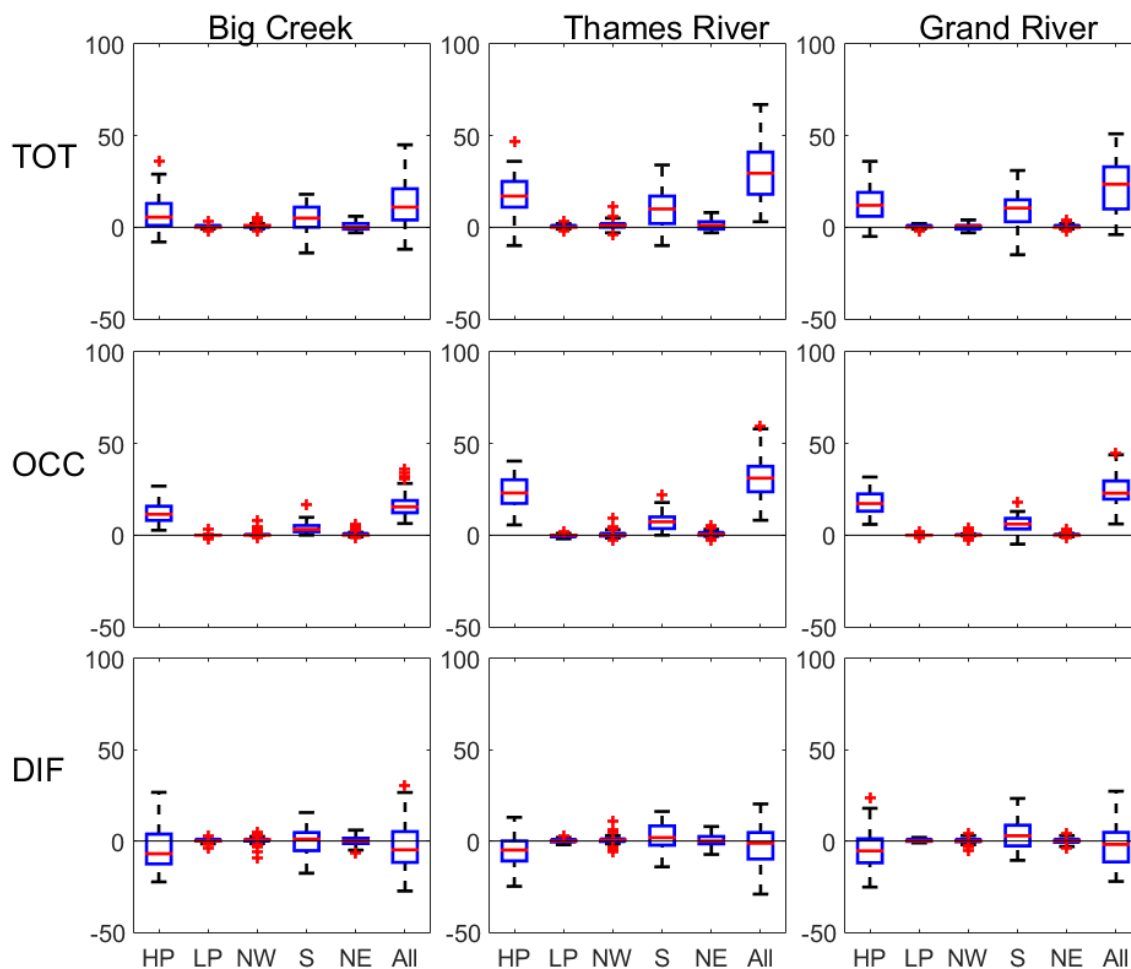
587 **Figure 8: Upper and mid panels: Distribution of observed (OBS) and simulated (CTL) streamflow corresponding to**  
 588 **all observed heavy rain and warm events. Lower panels: Distribution of simulated streamflow corresponding to all**  
 589 **simulated heavy rain and warm events (ENS). Boxes extend from the 25th to the 75th percentile, with a horizontal red**  
 590 **bar showing the median value. The whiskers are lines extending from each end of the box to the 1.5 interquartile range.**  
 591 **Plus signs correspond to outliers. The horizontal blue lines correspond to high flows (Average streamflow plus 3 times**  
 592 **the standard deviation).**





593

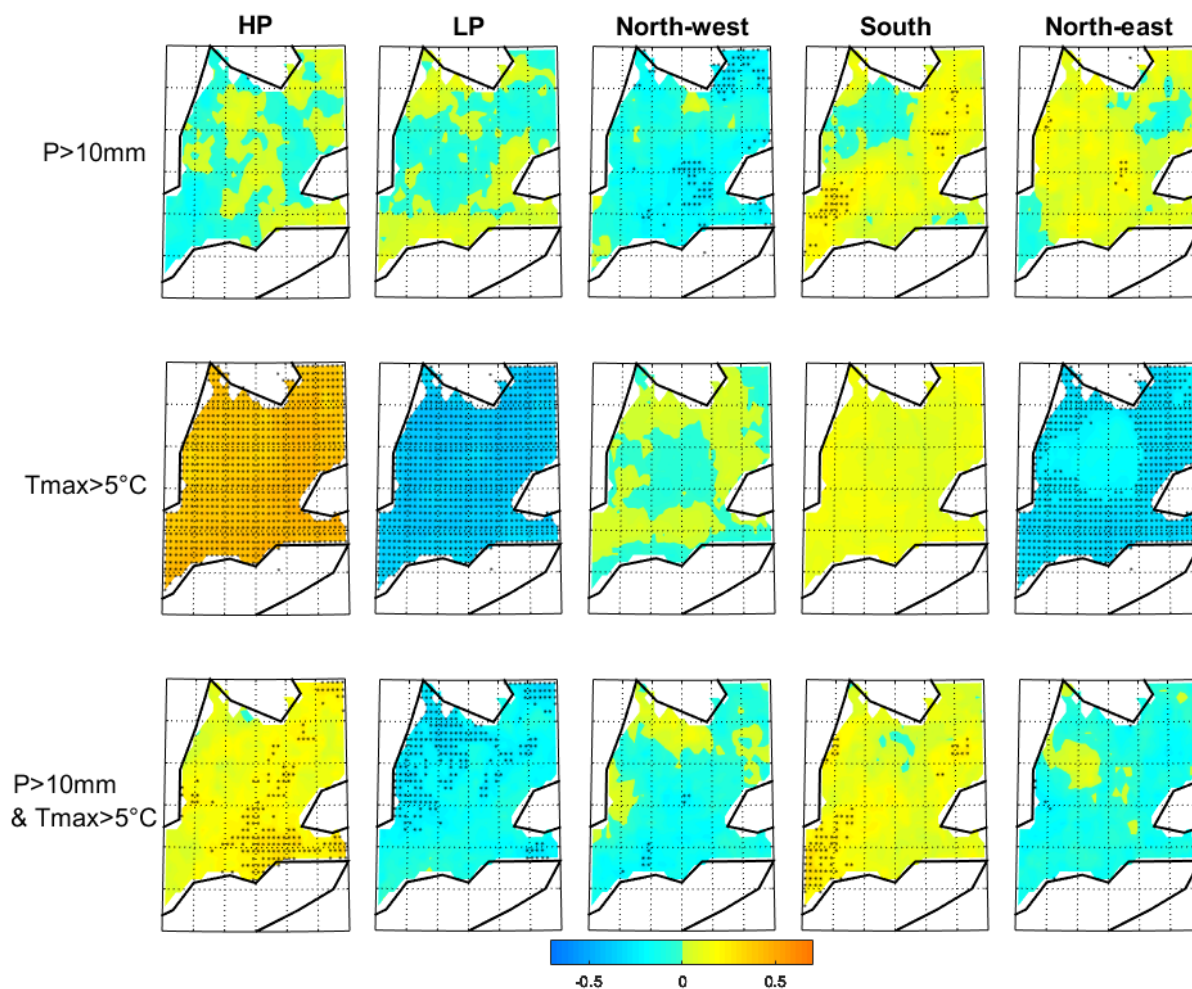
594 **Figure 9: DJF change in number of precipitation and warm events between the historical (1961-1990) and the future**  
 595 **period (2026-2055) for the 50 members CRCM5-LE average. The dotted lines represent the standard deviation of the**  
 596 **50-members CRCM5-LE simulated change in number of events.**



597

598 **Figure 10: upper panels: Distribution of change in number of high flows between 1961-1990 and 2026-2055 simulated**  
599 **from the 50 members of the ensemble (TOT). Mid panels: Distribution of theoretical change in number of high flows**  
600 **using the factor of change in number of heavy rain and warm events between 1961-1990 and 2026-2055 (OCC). Lower**  
601 **panels: TOT minus OCC (DIF). Boxes extend from the 25th to the 75th percentile, with a horizontal red bar showing**  
602 **the median value. The whiskers are lines extending from each end of the box to the 1.5 interquartile range. Plus signs**  
603 **correspond to outliers.**





604

605 **Figure 11: DJF inter-members correlations between change in occurrence of weather regimes and change in number**  
606 **of events between 1961-1990 and 2026-2055. Black points indicate a correlation significant at 95% according the**  
607 **Pearson's correlation table.**

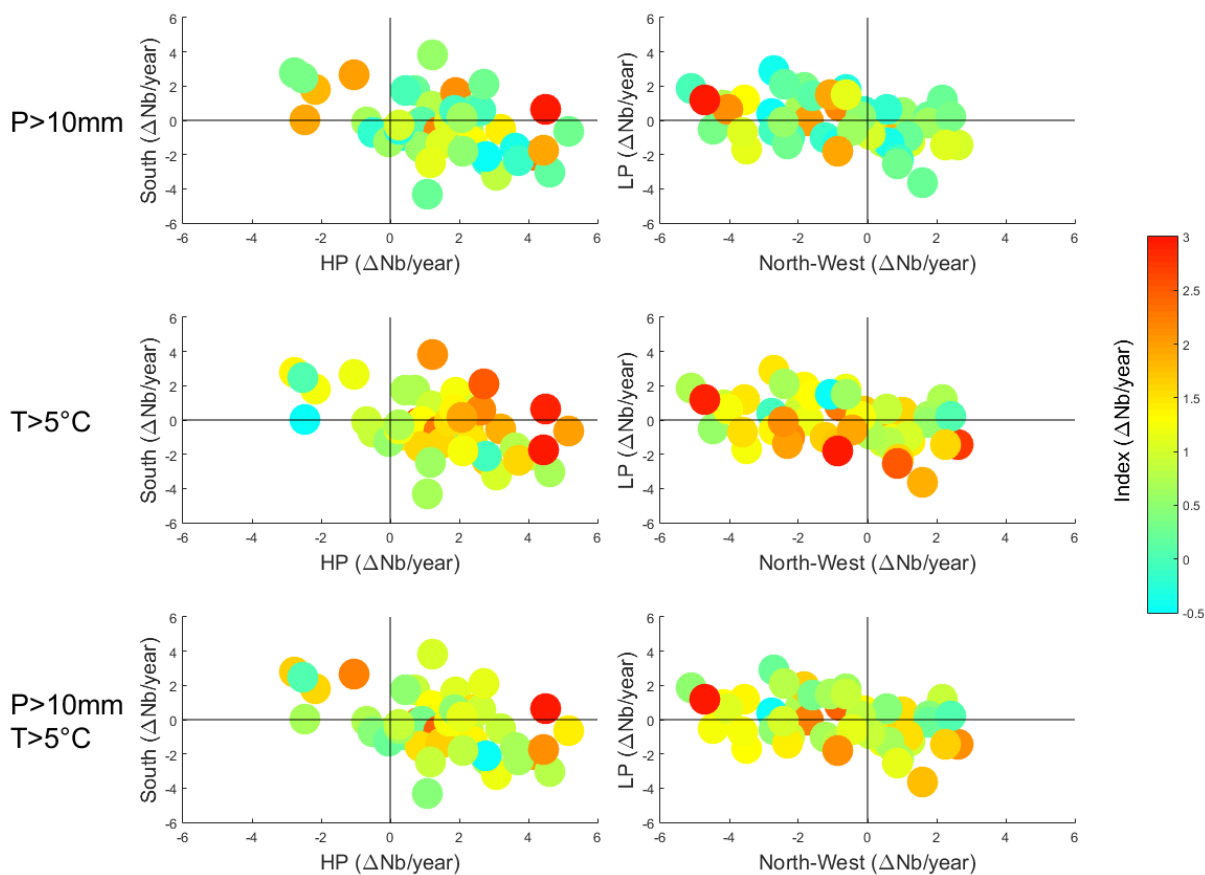
608

609

610

611

612



613

614 **Figure 12: DJF change in occurrences of regimes HP-South (left) and LP-north-West (right) in respect to change in**  
615 **number of precipitation and warm events (Colours) for each member of CRCM5-LE between 1961-1990 and 2026-**  
616 **2055.**

617

618

619

620

621

622

623

624



625 **Table 1: inter-members correlations between DJF change in occurrence of weather regimes and DJF change in number**  
 626 **of events between 1961-1990 and 2026-2055. Bold show correlations significant at 90% confidence level, a single**  
 627 **underline significant at 95% and double underline significant at 99% according to the Pearson's correlation table.**

	P>10mm					Tmax>5°C					P>10mm & Tmax>5°C				
	HP	LP	NW	S	NE	HP	LP	NW	S	NE	HP	LP	NW	S	NE
HP	-0.01	-0.01	-0.15	0.09	0.06	<u><b>0.43</b></u>	0.15	<u><b>0.32</b></u>	<u><b>0.55</b></u>	0.12	0.21	0.05	0.08	<u><b>0.35</b></u>	0.08
LP		0	-0.17	0.09	0.18		<u><b>-0.38</b></u>	<b>-0.26</b>	-0.13	<u><b>-0.46</b></u>		-0.21	<b>-0.23</b>	-0.01	-0.21
NW			-0.17	-0.06	-0.09			0	0.09	<b>-0.26</b>			-0.08	0.04	-0.08
S				0.12	0.18				0.13	-0.16				0.16	0.04
NE					0.10					<u><b>-0.28</b></u>					-0.10

628  
 629 **Table 2: inter-members correlations between DJF change in occurrence of weather regimes and DJF change in number**  
 630 **of high flows events between 1961-1990 and 2026-2055. Bold show correlations significant at 90% according to the**  
 631 **Pearson's correlation table.**

	Big Creek					Thames River					Grand River				
	HP	LP	NW	S	NE	HP	LP	NW	S	NE	HP	LP	NW	S	NE
HP	-0.13	<b>-0.25</b>	0.12	-0.09	-0.16	-0.08	-0.12	0.02	-0.02	-0.09	-0.10	-0.19	0	0.03	-0.10
LP		-0.18	0.15	-0.08	-0.16		-0.06	0.05	0.01	-0.07		-0.13	0	0.02	-0.10
NW			<b>0.26</b>	<b>0.25</b>	0.21			0.09	0.12	0.06			0.08	0.15	0.07
S				0.04	-0.03				0.06	-0.02				0.14	0.10
NE					-0.08					-0.04					-0.02

632